Published in final edited form as:

Mol Cell Endocrinol. 2018 December 15; 478: 1–9. doi:10.1016/j.mce.2018.06.016.

M_3-subtype muscarinic receptor activation stimulates intracellular calcium oscillations and aldosterone production in human adrenocortical HAC15 cells

Latha M. Malaiyandi[a], **Harsh Sharthiya**[a], **Nuntida Surachaicharn**[a], **Yara Shams**[b], **Mohammad Arshad**[a], **Chad Schupbach**[b], **Phillip G. Kopf**[b], and **Kirk E. Dineley**[b]

[a] Department of Anatomy, Midwestern University, Downers Grove, IL, 60515 USA

[b] Department of Pharmacology, Midwestern University, Downers Grove, IL, 60515 USA

Abstract

A previous body of work in bovine and rodent models shows that cholinergic agonists modulate the secretion of steroid hormones from the adrenal cortex. In this study we used live-cell Ca^{2+} imaging to investigate cholinergic activity in the HAC15 human adrenocortical carcinoma cell line. The cholinergic agonists carbachol and acetylcholine triggered heterogeneous Ca^{2+} oscillations that were strongly inhibited by antagonists with high affinity for the M3 muscarinic receptor subtype, while preferential block of M_1 or M_2 receptors was less effective. Acute exposure to carbachol and acetylcholine modestly elevated aldosterone secretion in HAC15 cells, and this effect was also diminished by M_3 inhibition. HAC15 cells expressed relatively high levels of mRNA for M_3 and M_2 receptors, while M_1 and M_5 mRNA were much lower. In conclusion, our data extend previous findings in non-human systems to implicate the M3 receptor as the dominant muscarinic receptor in the human adrenal cortex.

Keywords

Fluo-4; CHRM3; CHRM2; hypertension; tiotropium; methoctramine

1. Introduction

Aldosterone is the major mineralocorticoid hormone that regulates body electrolyte and fluid homeostasis (Fuller and Young, 2005). Synthesized and secreted from the glomerulosa layer of the adrenal cortex, aldosterone targets the distal tubule and collecting duct of the renal nephron, increasing the expression of basolateral Na^+-K^+ ATPase and luminal K^+ channels.

Corresponding Author: Kirk E. Dineley, PhD, Associate Professor of Pharmacology, Midwestern University, 555 31st Street, Downers Grove, IL 60515, kdineley@midwestern.edu, Office (630) 960-3907, Fax (630)515-6295.
lmalai@midwestern.edu, hshart@midwestern.edu, nsurachaicharn65@midwestern.edu, yshams11@midwestern.edu, marshad58@midwestern.edu, cschup@midwestern.edu, pkopf@midwestern.edu, kdinel@midwestern.edu

Declarations of interest: none

The principal direct consequences are Na^+ reclamation from and K^+ excretion into the ultrafiltrate, which in turn powerfully influences total body water and blood pressure. Proper maintenance of the aldosterone system is crucial: severe hypoaldosteronism typical of adrenal crisis can be fatal, while hyperaldosteronism is present in about 10% of primary hypertension cases and an even higher proportion of resistant hypertension cases that do not respond to drug treatment (Calhoun et al., 2008).

While serum K^+ and angiotensin II are the most important controllers of aldosterone in mammals, numerous other signalers have shown potential to modulate aldosterone production, including adrenocorticotropic hormone (ACTH), dopamine, atrial natriuretic peptide (ANP), endothelin-1, and acetylcholine (Bollag, 2014; Spät and Hunyady, 2004). The physiologic importance of these potential modulators is largely uncertain. A variety of studies using preparations derived from rodent and bovine adrenal cortex show that cholinergic agonists, such as acetylcholine or carbachol, mobilize intracellular Ca^{2+} and increase steroid secretion, presumably via activation of the M_3 muscarinic receptor subtype (Bollag et al., 1992; Jânossy et al., 1998; Kojima et al., 1986). Beyond this, the precise cellular mechanisms underlying cholinergic regulation of aldosterone production, and whether it is of physiological consequence, remains unclear.

The human adrenocortical carcinoma monoclonal cell line HAC15 is a subclone of the polyclonal H295R cell line (Wang and Rainey, 2012). HAC15 cells have pluripotential properties and as such can be induced to express all the enzymes necessary to manufacture the steroid hormones produced by the three functionally distinct layers of the adrenal cortex. This has made the HAC15 line an important and popular model for studying cellular and molecular mechanisms that govern steroid hormone production. A survey of recent literature shows that HAC15 cells have been used to explore the contrasting effects of thiazolidinedione drugs on cortisol and aldosterone production (Pan et al., 2014), the contribution of inwardly rectifying K^+ channel mutations in hyperaldosteronism (Hattangady et al., 2016; Oki et al., 2012), and to establish a role for Ca^{2+}/calmodulin-dependent protein kinase kinase in regulating steroidogenesis (Nanba et al., 2015). Thus, it is clear that a comprehensive understanding of the steroid biology of HAC15 cells is a worthwhile goal. Nonetheless, cholinergic regulation of steroid hormone synthesis and secretion has not been scrutinized in these cells or to our knowledge any other human cell model. In the following study, we investigated the relationship between cholinergic receptor activity, intracellular Ca^{2+} homeostasis, and aldosterone production in HAC15 cells.

2. Materials and Methods

2.1 Materials

Fluo-4, AM and cell culture reagents were purchased from Life Technologies, all other materials were from Sigma Aldrich. HAC15 cells were kindly provided by Dr. William Rainey. For ELISAs, the primary antibody against aldosterone was kindly provided by Dr. Celso Gomez-Sanchez.

2.2 Cell Culture

HAC15 cells were cultured in monolayers on collagen-coated surfaces, in growth media containing DMEM/F12, 10% Cosmic calf serum, 1% penicillin/streptomycin, 1% ITS + Premix and 0.1% gentamicin at 37°C, 5% CO_2. For microscopy experiments, 25mm or 18mm glass coverslips were coated with collagen one day prior to plating, and cells were plated in 6-well or 12-well plates at a density of 100,000 or 50,000 per well, respectively. After 2 days, media was replaced with steroidogenic media (same as growth medium but containing 0.1% Cosmic calf serum) and cells were used in experiments 1–2 weeks later.

2.3 Fluorescence Imaging

All imaging experiments were performed at room temperature on an IX70 Olympus fluorescence microscope equipped with a 40× oil-immersion objective (UAPO/340, ND = 1.35). The chamber was perfused with HEPES buffer containing (in mM): 140 NaCl, 0.5 KH_2PO_4, 3.1 KCl, 2 $NaHCO_3$, 0.9 $MgSO_4$, 5 HEPES, 5.5 glucose, 0.25 sulfinpyrazone, and 0.05 EGTA, pH adjusted to 7.4 with NaOH. Varying concentrations of drugs were diluted in buffer from 1000× stock solutions and perfused onto the cells to monitor dye response. Coverslips were incubated in 5μM Fluo-4 AM in HEPES buffer (supplemented with 5mg/mL BSA and 10μM *N,N,N′,N′-Tetrakis*(2-pyridylmethyl)ethylenediamine (TPEN) for 30 minutes at 25°C and then placed in a 500μL perfusion chamber and mounted onto the microscope stage. During experiments, cells were perfused with buffer at a rate of 5mL/min. Excitation light was provided by a xenon lamp-based Lambda LS stand-alone illuminator (Sutter Instruments). Incident light and emission signal was selected by a 480 nm band-pass excitation filter, a 500 nm dichromatic mirror, and a 520 nm long-pass emission filter. Images were captured with an LT Flash4.0 CMOS camera with HCImage acquisition software (Hamamatsu Photonics) in three-second increments. Fluorescence was quantified in a given field from 50–100 selected cells and represented as a ratio of fluorescence at any given time (F) divided by the starting, or baseline fluorescence (F_0). We did not convert fluorescence values to Ca^{2+} concentrations, due to the problematic nature of those calculations (Dineley et al., 2002).

2.4 ELISA

Aldosterone ELISA experiments followed methods previously described (Oki et al., 2013) with the following modifications. Cells were plated on collagen-coated 24-well plates at a density of 200,000/well. After 2 days, media was replaced with steroidogenic media. One-week-old cells were treated with carbachol, acetylcholine or angiotensin II for 60 minutes or 24 hours. In experiments with cholinergic inhibitors, cells were pretreated with antagonists for 10 minutes before and during the agonist treatment. Supernatant was collected, and aldosterone was measured using SuperSignal™ ELISA Pico Chemiluminescent Substrate, where luminescence was measured at 425 nm. After harvesting supernatant, cells were loaded with Hoechst 33342 (15μM) for 30 minutes at 37°C and fluorescence was measured at 460 nm, to ensure consistent cell density between wells.

2.5 Real-Time PCR

For muscarinic receptor expression experiments, cells were plated at 5,000,000 cells per T25 flask in growth media, replaced 2 days later with steroidogenic media and maintained in culture for 2 weeks. For examination of steroidogenic enzyme expression, HAC15 cells were plated on 6-well plates at a density of 1×10^6 cells/well. For both mRNA expression experiments, cells were harvested and RNA was purified using the MasterPure RNA purification kit (Epicenter). Thereafter, the RNA was converted to cDNA using MonsterScript 1st-Strand cDNA Synthesis kit (Epicenter). mRNA expression of muscarinic receptor subtypes (CHRM1, CHRM2, CHRM3, CHRM4, and CHRM5) was detected with manufacturer's instructions using the PerfeCTa SYBR Green SuperMix (VWR) and published primers at a concentration of 300nM (Table 1) (Mansfield et al., 2005). Muscarinic receptor values were normalized to the expression of the reference gene GAPDH, which was analyzed in parallel wells. In order to determine the relative expression of all the muscarinic receptors, the muscarinic receptor data was normalized to CHRM1. For steroidogenic enzymes, the reaction mixture was comprised of PerfeCTa qPCR ToughMix (Quantabio, Beverly, MA), 500nM for each primer (see Table 1), 250nM for each probe, and 37.5 ng cDNA/well. PrimeTime qPCR probe-based assays (Integrated DNA Technologies, Coralville, IA) were used to analyze expression of each gene of interest in duplex with the reference gene GAPDH using probe fluorophores of FAM and HEX fluorophores, respectively. Because the primers for CHRM4 did not yield acceptable levels of amplification efficiency, our experiments did not address CHRM4 expression. Tolerance for all other primer sets was 90–110%. Real-time data were obtained during the extension phase and critical threshold cycle values were calculated at the log phase of each gene amplification curve.

2.6 Statistical Analyses

All experiments were repeated at least three times using cells from at least three different culture preparations. All data processing and statistical analysis was performed using GraphPad Prism version 7.01 for Windows (GraphPad Software). The frequency of oscillatory activity for each cell was quantified by counting the number of peaks, where a peak was defined by any event where fluorescence, F, exceeded baseline fluorescence, F0, by a factor of two. Area under the curve (AUC) measurements were also calculated for all peaks, using Prism built-in functions. Each cell was considered a sample and each microscopy coverslip yielded approximately 50–100 cells. The bars in the summary graphs are represented as the mean number of peaks with 95% CI. We summarized AUC data by one of two methods. We calculated the total area of all peaks for each cell, and we calculated the average area of the individual peaks, for each cell. Both are reported as mean with 95% CI. Aldosterone values were calculated as mean pg/mL ± SEM, represented as fold increase from basal levels, from three replicates each from at least three different culture passages.

For figures 4, 6, 7, S1, and S2, comparisons were made using one-way ANOVA followed by Dunnett's post-test. Other statistical comparisons used Student's t-test. p value < 0.05 was regarded as significant.

3. Results

Previous studies in bovine and rodent adrenocortical models have identified cholinergic receptor control over steroid production that is linked to Ca^{2+} mobilization. To search for similar activity in the HAC15 human cell line, we began with live-cell imaging experiments using the Ca^{2+}-sensitive fluorophore Fluo-4. Fluo-4 is particularly useful in situations where high Ca^{2+} sensitivity is helpful due to its bright fluorescence emission and superior accumulation inside cells (Gee et al., 2000) (Figure 1A). We found that HAC15 cells exhibited Ca^{2+} oscillations when stimulated with carbachol, the stable synthetic analogue of acetylcholine, in a concentrationdependent fashion (Figure 3A). Figure 1 shows a typical sequence of images from the same cells, sampled in three-second intervals during the carbachol treatment (10μM). Many of the cells experienced oscillations (e.g. those in the circled groups) while others remain quiescent. Figures 1B-D depict the heterogeneity of the responses.

The mobilized Ca^{2+} was largely of intracellular origin because oscillations persisted when Ca^{2+} was removed from the extracellular superfusate (Figure 2B). However, a more pronounced rundown effect over time is apparent in the Ca^{2+}-free conditions. We further investigated the source of intracellular Ca^{2+} using classic inhibitors of ER and mitochondrial storage mechanisms. We found that carbachol-induced Ca^{2+} oscillations were primarily derived from IP_3-mediated ER Ca^{2+} release, while little was attributable to ryanodine-sensitive stores, or mitochondrial Ca^{2+} storage pathways (Supplementary Figures 1 and 2). This is consistent with PLC-IP_3 second messenger pathways associated with excitatory muscarinic receptors, and moreover is a classic demonstration of the role that store-operated Ca^{2+} mechanisms occupy in resupplying the small amounts of Ca^{2+} lost from the cell with each cycle of release and recapture (Dupont et al., 2011). In any case, because extracellular Ca^{2+} was not critical for the muscarinic receptor-mediated oscillations, and because it could contribute to confounding intracellular transients arising from other mechanisms, our imaging experiments omitted Ca^{2+} from the superfusate unless otherwise noted.

The extent of oscillation in each cell was quantified as the number of peaks that rose at least two-fold above baseline fluorescence. The frequency histogram in Figure 2C depicts the large degree of heterogeneity in the population: the average number of Ca^{2+} peaks per cell was 5.77 and 5.25 in the presence and absence of extracellular Ca^{2+}, respectively. However, between 12–14% percent of cells did not respond at all, while 16–20% of cells exhibited more than 10 peaks (and as many as 25) during the five-minute period of stimulus. Cholinergic oscillations were entirely attributable to muscarinic subtypes, because the activity was also triggered by acetylcholine (ACh) and bethanechol, but not by nicotine (Figures 3B-D). For comparison, angiotensin II also increased intracellular Ca^{2+}. However, the transients differed markedly from cholinergic-mediated oscillations, in that the angiotensin II responses manifested uniformly in all cells as a monotonic transient that did not oscillate (Figure 3E). Previous work in primary glomerulosa cells showed that picomolar concentrations of angiotensin II could elicit Ca^{2+} oscillations, while nanomolar amounts caused larger transients that plateaued and did not oscillate (Quinn et al., 1988; Rössig et al., 1996). However we were unable to observe oscillations with any concentration of angiotensin II (10pM-100nM). This discrepancy might be explained by a lack of certain

ionic channels in the HAC15 line, compared to primary cells, that are necessary for angiotensin II-induced oscillations (Hu et al., 2012). If so, this deficiency clearly does not prevent cholinergic oscillations.

We next sought to determine which of the five muscarinic subtypes, M_1-M_5, regulate the Ca^{2+} response, using a panel of muscarinic receptor antagonists with varying subtype preferences: atropine (high affinity but non-selective), tiotropium and darifenacin (M3-preferring), pirenzepine (M_1-preferring) and methoctramine (M_2-preferring) (Casarosa et al., 2009; Hegde et al., 1997). For these assays, the inhibitor was included in the superfusate for three minutes before and during the five-minute stimulation with carbachol or ACh. Tiotropium at just 1μM eliminated virtually all carbachol-induced activity (Figure 4A). Figures 4B and C summarize trials of carbachol or acetylcholine (10μM) in the presence of muscarinic inhibitors (1μM), with data expressed as the average number of peaks in the cell population. We also carried out detailed concentration response trials (Figure 4D) for tiotropium, darifenacin, pirenzepine, and methoctramine, in the presence of carbachol (10μM). The extent of inhibition was expressed as the percentage of responding cells (i.e. any cell that showed at least one Ca^{2+} peak ≥twice baseline fluorescence was considered a responder). These curves allowed us to infer IC_{50} values for each of the subtype-preferring muscarinic blockers (see Table 2). Both of the high-affinity, M_3-preferring blockers tiotropium and darifenacin potently suppressed oscillations (IC_{50} = 0.002μM and 0.065μM, respectively). Moderate inhibition was achieved by the M_1-preferring antagonist pirenzepine (IC_{50} = 0.69μM), whereas the M_2-preferring blocker methoctramine was comparatively weak (IC_{50} = 4.27μM).

To compare the Ca^{2+} signaling dynamics for different steroidogenic stimuli, we exposed HAC15 cells to angiotensin II (100nM) for five minutes (Figures 5A-C). Similar to the data in Figure 3E, this elicited robust Ca^{2+} changes that took the form of a single, large, and relatively uniform transient that featured little if any oscillatory activity (Figure 5A). Atropine (1 μM) had no effect on the frequency of peaks per cell (Figure 5B). We also calculated the total area under the curve for all peaks in each cell, for both carbachol and angiotensin II conditions. This showed that the numerous small transients elicited by carbachol (10μM) constitute a total Ca^{2+} load that is roughly equal to the Ca^{2+} change caused by angiotensin II (100nM). However, the individual peaks in the carbachol-treated cells were on average about half the area of the average angiotensin II peak (Figure 5C).

Previous studies in models derived from bovine and rodent tissue showed that muscarinic receptor activation can stimulate the production of steroids, albeit to a lesser extent than can be achieved with angiotensin II. We used an ELISA-based aldosterone assay to determine the effects of carbachol and acetylcholine on HAC15 steroid production (Figure 6). Consistent with previous reports, we found that treatment with acetylcholine or carbachol (100μM) for one hour acutely increased aldosterone secretion, but angiotensin II (100nM) had no effect (Figure 6A). In comparison, angiotensin II for 24 hours increased aldosterone production by at least 10-fold, at which time point the effect of the cholinergic agonists had dissipated compared to the one-hour treatment (Figure 6B). In either time course, tiotropium (1μM) blocked aldosterone production, but pirenzepine and methoctramine did not. The antimuscarinics had no effect on angiotensin IIinduced aldosterone production.

We next asked if the cholinergic agonists caused any changes in the aldosterone synthesis machinery. We used RT-PCR to determine changes in CYP11B1, CYP11B2, and StAR (Table 3). We found that 24-hour treatment with carbachol or acetylcholine (100μM) caused modest yet statistically significant upregulation of CYP11B1 and CYP11B2, but did not change StAR. In contrast, angiotensin II (100nM) increased the two CYPs by more than 4-fold, and 15-fold, respectively.

Lastly, we used quantitative RT-PCR to determine the relative mRNA expression for the different muscarinic subtypes (Figure 7). Consistent with our pharmacological data, we found that M_3 message was most abundant, at levels roughly 7.5-fold higher than the least abundant M_1 message. M2 mRNA was also relatively abundant, while M5 was considerably lower. We were unable to detect mRNA for M_4.

4. Discussion

Our data build upon previous studies in bovine and rodent models to support the conclusion that the M_3 muscarinic receptor is the dominant cholinergic receptor in human adrenal glomerulosa cells. In our experiments, carbachol, acetylcholine, and bethanechol, but not nicotine, stimulated intracellular Ca^{2+} oscillations. These were largely attributed to cyclical release and recapture of intracellular ER stores, because oscillatory activity persisted in the absence of extracellular Ca^{2+} and was markedly inhibited by thapsigargin and caffeine. Muscarinic receptor antagonists possessing high affinity for the M3 subtype inhibited oscillations nearly completely. Similarly, both acetylcholine and carbachol increased aldosterone production, albeit modestly, and this increase was most effectively diminished by a high affinity, M_3-preferring inhibitor. Finally, RT-PCR suggests that the mRNA for the M_3 subtype is the most abundant muscarinic receptor transcript in HAC15 cells.

Molecular biology has revealed the presence of five distinct muscarinic receptor subtypes in vertebrates, designated M_1-M_5 (Eglen, 2005). All are members of the G-protein coupled receptor superfamily and all are found in both CNS and the periphery, but with markedly different patterns of distribution. The activity of parasympathetic effectors is dominated by M_3 and M_2 subtypes. M_3 function is perhaps best understood in smooth muscle, particularly in the airways, bladder, and GI, where activation is linked to PLC-IP_3 pathways that mobilize Ca^{2+} and stimulate contraction. M_2 receptors are well delineated in the heart, where they slow pacemaker cell activity via inhibition of adenylate cyclase, reduction of cyclic nucleotides, activation of K^+ channels, and inhibition of Ca^{2+} channels. In tissues possessing multiple muscarinic subtypes, determination of the respective functional contributions is hampered by a lack of truly selective modulators, which is a consequence of the close structural homology shared between all the muscarinic receptors, particularly at their ACh binding sites (Eglen, 2005). In our experiments, we used the high-affinity antagonists darifenacin and tiotropium to block M_3 receptors. Darifenacin affinity for M_3 is about 70-fold higher than M_2. Tiotropium is only about three-fold more selective based on affinity alone but is thought to be functionally selective because it remains bound to the M_3 receptor for a much longer duration (Tautermann et al., 2013). We found that both darifenacin and tiotropium potently and effectively silenced Ca^{2+} oscillations triggered by acetylcholine or carbachol, with IC_{50} values of 65 and 2.0nM, respectively. By comparison,

the M_1-preferring antagonist pirenzepine was a moderate inhibitor of Ca^{2+} oscillations (IC_{50} = 690nM). The M_2-preferring methoctramine was weaker yet (IC_{50} = 4.27μM), silencing only about 60% of the cells even at the highest concentration tested (10μM).

The heterogeneous intracellular Ca^{2+} response to muscarinic agonists differs from the effects we observed with angiotensin II, which at 100nM caused a single, large and long-lasting Ca^{2+} transient in virtually 100% of cells. By comparison, muscarinic agonists produced a highly diverse set of responses. In Ca^{2+}-free conditions, about 12% of cells did not respond at all, while 16% displayed more than 10 peaks, and a small percentage displayed more than 20. To gauge the total peak activity of each cell, AUC for all peaks in a cell were summated. This revealed that the total AUC per cell was not different between the angiotensin II and carbachol conditions. In other words, the many small transients elicited by a modest concentration of muscarinic agonist (10μM), when added together, constituted a total Ca^{2+} load roughly equal to that achieved by a relatively generous concentration of angiotensin II (100nM). This suggests that perhaps the relative impotence of muscarinic activity in stimulating aldosterone production lies not in an inability to mobilize sufficient amounts of Ca^{2+}, but rather the failure to mobilize it simultaneously. From that, it seems reasonable to suggest that the sustained cytosolic Ca^{2+} load of angiotensin II would be more conducive to the mitochondrial Ca^{2+} accumulation that appears to be critical for stimulating aldosterone synthesis (Szanda et al., 2012; Wiederkehr et al., 2011).

Ca^{2+} oscillations are a common phenomenon triggered by numerous GPCRs and documented in a wide variety of cell types (Dupont et al., 2011). The current view regards the oscillatory mechanism as a finely tuned mode of intracellular signaling that is (*i*) responsive to low levels of extracellular ligands, and (*ii*) possesses high signal-to-noise, because true oscillatory activity can be easily distinguished from random fluctuations. While the magnitude of Ca^{2+} change with a single oscillation is small, the tight juxtaposition of ER and mitochondria compartments is thought to serve as an intracellular synapse that facilitates Ca^{2+}-mediated communication between the two organelles (Csordás et al., 2006). Given the central role of mitochondria in steroidogenesis, such thinking is particularly intriguing in the adrenal cortex. Nevertheless, the specific function of Ca^{2+} oscillations for any cell type remains speculative. A potentially interesting insight gleaned from the present work is that oscillations become more frequent in HAC15 cells that have been growing in steroidogenic media, as opposed to those kept in growth media (Supplementary Figure 3). This suggests that M_3 receptor control over Ca^{2+} becomes more prominent as the cells become poised toward steroidogenesis.

Both acetylcholine and carbachol also stimulated aldosterone secretion, but weakly compared to angiotensin II. Treatment with cholinergic agonist for one-hour was sufficient to significantly increase aldosterone secretion. After 24 hours, aldosterone still trended higher, but was not significantly different from control, due to the fact that HAC15 cells constantly secrete steroid hormones, regardless of stimulus. In trials using muscarinic receptor antagonists, we found that tiotropium markedly inhibited aldosterone production induced by ACh or carbachol, while pirenzepine and methoctramine did not. Thus, both Ca^{2+} oscillation and aldosterone secretion were inhibited most effectively by an M_3-preferring antagonist. The rapid effects of cholinergic agonists on aldosterone production

suggests that muscarinic receptor activation accelerates the release of aldosterone that is already synthesized. However, with longer treatments, cholinergic agonists also appear to moderately upregulate some components of the aldosterone synthesis pathway. These data contrast markedly with the effect of angiotensin II, which had no acute effect on aldosterone secretion, but in the 24-hour treatment greatly elevated both aldosterone production and CYP11B1 and CYP11B2 expression.

A number of previous reports provided evidence for cholinergic enhancement of cortisol secretion in fasiculata preparations. In some of the earliest work in mammalian systems, Hadjian and colleagues used bovine cortical membranes and fasiculata cells to show that acetylcholine stimulated cortisol production, but to a much weaker degree compared to ACTH (Hadjian et al., 1984; 1982; 1981). This activity was attributed to muscarinic receptors that stimulated phosphoinositide turnover and Ca^{2+} mobilization but did not alter the cyclic nucleotide pool. Subsequent reports using muscarinic agonists in bovine cells suggested that ACh-mediated phosphoinositide turnover and cortisol production was most consistent with M_3 receptors coupled to phospholipase C (Clyne et al., 1994; Jánossy et al., 1999; Walker et al., 1990). Other work explained the weak steroidogenic effect of carbachol as a consequence of fast internalization of the M_3 receptor (Jánossy et al., 2001). Fewer studies have been carried out in glomerulosa models, but their findings are broadly similar: in bovine glomerulosa cells, cholinergic agonists stimulated aldosterone production via mechanisms that relied on phosphoinositide hydrolysis and mobilization of intracellular Ca^{2+} (Kojima et al., 1986). The weak induction of aldosterone production by carbachol, relative to angiotensin II, was ascribed to inadequate mobilization of intracellular Ca^{2+}. Later work by Bollag and colleagues suggested that an important distinction between angiotensin II and carbachol was the tendency of carbachol to induce the formation of a comparatively short-lived species of DAG that declines rapidly after agonist removal, possibly because carbachol activation of phospholipase D is transient (Bollag et al., 1992; Jung et al., 1998).

While all the cell-based results, including data in this report, point to the M_3 receptor as the most functionally important muscarinic subtype, at least within the adrenal cortex, a far more complicated picture emerges from studies of physiologically intact systems. In microperfusion experiments with rat capsule-glomerulosa preparations, the M_1 antagonist pirenzepine *enhanced* aldosterone. This was presumed to result from inhibition of M1 autoreceptors that inhibit ACh release from parasympathetic postganglionic axons terminating in the cortex (Jánossy et al., 1998). Interestingly, the authors noted that cholinergic agonists increased aldosterone production in a few samples, but the overall effect in the entire group did not reach statistical significance. These disparate observations raise the possibility that cholinergic activity in the adrenal cortex may differ profoundly between individuals. Another study in mice showed that corticosterone levels are increased five-fold by the mixed modulator BuTAC, which activates M2 receptors while blocking M_3 (Watt et al., 2013). This enhancement is lost in mice with targeted disruption of the M_2 receptor (Hemrick-Luecke, 2002). Unfortunately, that report did not address the location in the HPA axis where this effect occurs. In human males, intravenous atropine inhibited aldosterone secretion stimulated by angiotensin II and metoclopramide, but not by ACTH (Stern et al., 1989). These studies are interesting in their own right, but when considered together they do

not yield a consistent and informative interpretation of cholinergic influence on the aldosterone system.

Intriguingly, our RT-PCR data found M_2 mRNA present at levels on par with M_3. This stands in contrast to one of the aforementioned bovine studies which found mRNA for M_3, but not for M_2 or M_4 (Jánossy et al., 1999). (Because the sequences were unknown at the time, it was not possible for the authors to test for bovine M_1 or M_5.) In our Ca^{2+} imaging experiments, the M_2-preferring blocker methoctramine inhibited oscillations only at high concentrations. We assume this effect arises from methoctramine block at M_3 receptors (methoctramine affinity for M_3 is roughly 800nM). Consistent with this are numerous previous results in both glomerulosa and fasiculata cells from rat or cow which found that muscarinic activation did not change cyclic nucleotides, as would be expected with classic M_2 second messenger pathways which are known to inhibit adenylate cyclase. However, these data do not rule out a possible role for M_2 receptors in human cortical cells, and it is tempting to speculate that the aforementioned BuTAC influences steroid production via some direct action on cortical M_2 receptors.

5. Conclusions

Taken together, our results extend to a human glomerulosa model previous findings that identify the M_3 muscarinic receptor as the most important subtype in cholinergic modulation of aldosterone synthesis and secretion. We also suggest that the relatively weak steroidogenic effect associated with cholinergic agonists is partly attributable to the pulsatile nature of Ca^{2+} transients triggered by muscarinic receptor activation. Further experiments are needed, particularly in regard to a possible role for the M_2 receptor.

Supplementary Material

Refer to Web version on PubMed Central for supplementary material.

Acknowledgments

We extend thanks to the reviewers whose critical feedback improved this manuscript, and also to Drs. Annette Gilchrist, Ian Reynolds, and Rafael Mejia-Alvarez for their helpful discussions.

Funding: This work was supported by the National Institutes of Health (HL-124326, PGK) and Midwestern University's Walczak Research Award and other intramural funds. The funding sources had no involvement in study design; in the collection, analysis and interpretation of data; in the writing of the report; or in the decision to submit the article for publication.

6. References

Bollag WB, 2014 Regulation of aldosterone synthesis and secretion. Compr Physiol 4, 1017–1055. doi:10.1002/cphy.c130037 [PubMed: 24944029]

Bollag WB, Barrett PQ, Isales CM, Liscovitch M, Rasmussen H, 1992 Signal transduction mechanisms involved in carbachol-induced aldosterone secretion from bovine adrenal glomerulosa cells. Molecular and Cellular Endocrinology 86, 93–101. [PubMed: 1511782]

Calhoun DA, Jones D, Textor S, Goff DC, Murphy TP, Toto RD, White A, Cushman WC, White W, Sica D, Ferdinand K, Giles TD, Falkner B, Carey RM, American Heart Association Professional Education Committee, 2008 Resistant hypertension: diagnosis, evaluation, and treatment: a scientific statement from the American Heart Association Professional Education Committee of the

Council for High Blood Pressure Research. Circulation. doi:10.1161/CIRCULATIONAHA.108.189141

Casarosa P, Bouyssou T, Germeyer S, Schnapp A, Gantner F, Pieper M, 2009 Preclinical evaluation of long-acting muscarinic antagonists: comparison of tiotropium and investigational drugs. Journal of Pharmacology and Experimental Therapeutics 330, 660–668. doi: 10.1124/jpet.109.152470 [PubMed: 19478135]

Clyne CD, Walker SW, Nicol MR, Williams BC, 1994 The M3 muscarinic receptor mediates acetylcholine-induced cortisol secretion from bovine adrenocortical zona fasciculata/reticularis cells. Biochem. Pharmacol 47, 1145–1150. [PubMed: 8161343]

Csordás G, Renken C, Várnai P, Walter L, Weaver D, Buttle KF, Balla T, Mannella CA, Hajnóczky G, 2006 Structural and functional features and significance of the physical linkage between ER and mitochondria. J. Cell Biol 174, 915–921. doi:10.1083/jcb.200604016 [PubMed: 16982799]

Dineley KE, Malaiyandi LM, Reynolds IJ, 2002 A reevaluation of neuronal zinc measurements: artifacts associated with high intracellular dye concentration. Mol. Pharmacol 62, 618–627. [PubMed: 12181438]

Dupont G, Combettes L, Bird GS, Putney JW, 2011 Calcium oscillations. Cold Spring Harb Perspect Biol 3, a004226–a004226. doi:10.1101/cshperspect.a004226 [PubMed: 21421924]

Eglen RM, 2005 Muscarinic receptor subtype pharmacology and physiology. Prog Med Chem 43, 105–136. doi: 10.1016/S0079-6468(05)43004-0 [PubMed: 15850824]

Fuller PJ, Young MJ, 2005 Mechanisms of mineralocorticoid action. Hypertension 46, 1227–1235. doi:10.1161/01.HYP.0000193502.77417.17 [PubMed: 16286565]

Gee KR, Brown KA, Chen WN, Bishop-Stewart J, Gray D, Johnson I, 2000 Chemical and physiological characterization of fluo-4 Ca(2+)-indicator dyes. Cell Calcium 27, 97–106. doi: 10.1054/ceca.1999.0095 [PubMed: 10756976]

Hadjian AJ, Culty M, Chambaz EM, 1984 Stimulation of phosphatidylinositol turnover by acetylcholine, angiotensin II and ACTH in bovine adrenal fasciculata cells. Biochim. Biophys. Acta 804, 427–433. [PubMed: 6087924]

Hadjian AJ, Guidicelli C, Chambaz EM, 1982 Cholinergic muscarinic stimulation of steroidogenesis in bovine adrenal cortex fasciculata cell suspensions. Biochim. Biophys. Acta 714, 157–163. [PubMed: 6275905]

Hadjian AJ, Ventre R, Chambaz EM, 1981 Cholinergic muscarinic receptors in bovine adrenal cortex. Biochemical and Biophysical Research Communications 98, 892–900. [PubMed: 7225130]

Hattangady NG, Karashima S, Yuan L, Ponce-Balbuena D, Jalife J, Gomez-Sanchez CE, Auchus RJ, Rainey WE, Else T, 2016 Mutated KCNJ5 activates the acute and chronic regulatory steps in aldosterone production. Journal of Molecular Endocrinology 57, 1–11. doi:10.1530/JME-15-0324 [PubMed: 27099398]

Hegde SS, Choppin A, Bonhaus D, Briaud S, Loeb M, Moy TM, Loury D, Eglen RM, 1997 Functional role of M2 and M3 muscarinic receptors in the urinary bladder of rats in vitro and in vivo. Br. J. Pharmacol 120, 1409–1418. doi:10.1038/sj.bjp.0701048 [PubMed: 9113359]

Hemrick-Luecke SK, 2002 Muscarinic Agonist-Mediated Increases in Serum Corticosterone Levels Are Abolished in M2 Muscarinic Acetylcholine Receptor Knockout Mice. Journal of Pharmacology and Experimental Therapeutics 303, 99–103. doi:10.1124/jpet.102.036020 [PubMed: 12235238]

Hu C, Rusin CG, Tan Z, Guagliardo NA, Barrett PQ, 2012 Zona glomerulosa cells of the mouse adrenal cortex are intrinsic electrical oscillators. The Journal of clinical investigation 122, 2046–2053. doi:10.1172/JCI61996 [PubMed: 22546854]

Jânossy A, Li JY, Saez JM, 1999 Characterisation of the muscarinic receptor subtype M3 in the bovine zona fasciculata-reticularis cells by receptor binding, mRNA and functional studies. J. Endocrinol 163, 329–336. [PubMed: 10556783]

Jánossy A, Orsó E, Szalay KS, Jurânyi Z, Beck M, Vizi ES, Vinson GP, 1998 Cholinergic regulation of the rat adrenal zona glomerulosa. J. Endocrinol 157, 305–315. [PubMed: 9659294]

Jánossy A, Saez JM, Li JY, 2001 Carbachol induces homologous steroidogenic refractoriness of bovine fasciculata-reticularis cells. Molecular and Cellular Endocrinology 172, 147–155. [PubMed: 11165048]

Jung E, Betancourt-Calle S, Mann-Blakeney R, Foushee T, Isales CM, Bollag WB, 1998 Sustained phospholipase D activation in response to angiotensin II but not carbachol in bovine adrenal glomerulosa cells. Biochem. J 330 (Pt 1), 445–451. [PubMed: 9461542]

Kojima I, Kojima K, Shibata H, Ogata E, 1986 Mechanism of cholinergic stimulation of aldosterone secretion in bovine adrenal glomerulosa cells. Endocrinology 119, 284–291. doi:10.1210/endo-119-1-284 [PubMed: 2873026]

Mansfield KJ, Liu L, Mitchelson FJ, Moore KH, Millard RJ, Burcher E, 2005 Muscarinic receptor subtypes in human bladder detrusor and mucosa, studied by radioligand binding and quantitative competitive RT-PCR: changes in ageing. Br. J. Pharmacol 144, 1089–1099. doi: 10.1038/sj.bjp.0706147 [PubMed: 15723094]

Nanba K, Chen A, Nishimoto K, Rainey WE, 2015 Role of Ca(2+)/calmodulin-dependent protein kinase kinase in adrenal aldosterone production. Endocrinology 156, 1750–1756. doi:10.1210/en.2014-1782 [PubMed: 25679868]

Oki K, Kopf PG, Campbell WB, Luis Lam M, Yamazaki T, Gomez-Sanchez CE, Gomez-Sanchez EP, 2013 Angiotensin II and III metabolism and effects on steroid production in the HAC15 human adrenocortical cell line. Endocrinology 154, 214–221. doi:10.1210/en.2012-1557 [PubMed: 23221601]

Oki K, Plonczynski MW, Luis Lam M, Gomez-Sanchez EP, Gomez-Sanchez CE, 2012 Potassium channel mutant KCNJ5 T158A expression in HAC-15 cells increases aldosterone synthesis. Endocrinology 153, 1774–1782. doi:10.1210/en.2011-1733 [PubMed: 22315453]

Pan Z-Q, Xie D, Choudhary V, Seremwe M, Tsai Y-Y, Olala L, Chen X, Bollag WB, 2014 The effect of pioglitazone on aldosterone and cortisol production in HAC15 human adrenocortical carcinoma cells. Molecular and Cellular Endocrinology 394, 119–128. doi:10.1016/j.mce.2014.07.007 [PubMed: 25038520]

Quinn SJ, Williams GH, Tillotson DL, 1988 Calcium oscillations in single adrenal glomerulosa cells stimulated by angiotensin II. Proc. Natl. Acad. Sci. U.S.A 85, 5754–5758. [PubMed: 3399509]

Rössig L, Zólyomi A, Catt KJ, Balla T, 1996 Regulation of angiotensin II-stimulated Ca2+ oscillations by Ca2+ influx mechanisms in adrenal glomerulosa cells. J. Biol. Chem 271, 22063–22069. [PubMed: 8703014]

Spät A, Hunyady L, 2004 Control of aldosterone secretion: a model for convergence in cellular signaling pathways. Physiol. Rev 84, 489–539. doi:10.1152/physrev.00030.2003 [PubMed: 15044681]

Stern N, Pullen W, Plasko R, Eggena P, Tuck ML, 1989 Evidence for cholinergic modulation of aldosterone secretion in man. J. Clin. Endocrinol. Metab 69, 294–298. doi:10.1210/jcem-69-2-294 [PubMed: 2568995]

Szanda G, Rajki A, Spät A, 2012 Control mechanisms of mitochondrial Ca(2+) uptake - feed-forward modulation of aldosterone secretion. Molecular and Cellular Endocrinology 353, 101–108. doi: 10.1016/j.mce.2011.08.042 [PubMed: 21924321]

Tautermann CS, Kiechle T, Seeliger D, Diehl S, Wex E, Banholzer R, Gantner F, Pieper MP, Casarosa P, 2013 Molecular basis for the long duration of action and kinetic selectivity of tiotropium for the muscarinic M3 receptor. J. Med. Chem 56, 8746–8756. doi:10.1021/jm401219y [PubMed: 24088171]

Walker SW, Strachan MW, Lightly ER, Williams BC, Bird IM, 1990 Acetylcholine stimulates cortisol secretion through the M3 muscarinic receptor linked to a polyphosphoinositide-specific phospholipase C in bovine adrenal fasciculata/reticularis cells. Molecular and Cellular Endocrinology 72, 227–238. [PubMed: 1963158]

Wang T, Rainey WE, 2012 Human adrenocortical carcinoma cell lines. Molecular and Cellular Endocrinology 351, 58–65. doi:10.1016/j.mce.2011.08.041 [PubMed: 21924324]

Watt ML, Rorick-Kehn L, Shaw DB, Knitowski KM, Quets AT, Chesterfield AK, McKinzie DL, Felder CC, 2013 The muscarinic acetylcholine receptor agonist BuTAC mediates antipsychotic-like effects via the M4 subtype. Neuropsychopharmacology 38, 2717–2726. doi: 10.1038/npp.2013.186 [PubMed: 23907402]

Wiederkehr A, Szanda G, Akhmedov D, Mataki C, Heizmann CW, Schoonjans K, Pozzan T, Spät A, Wollheim CB, 2011 Mitochondrial matrix calcium is an activating signal for hormone secretion. Cell Metab. 13, 601–611. doi:10.1016/j.cmet.2011.03.015 [PubMed: 21531342]

Highlights:

- Cholinergic agonists trigger intracellular Ca^{2+} oscillations via M_3 receptors
- Muscarinic agonists acutely elevate aldosterone secretion via M_3 receptors
- Muscarinic receptor activation modestly induces steroidogenic CYPs in HAC15 cells

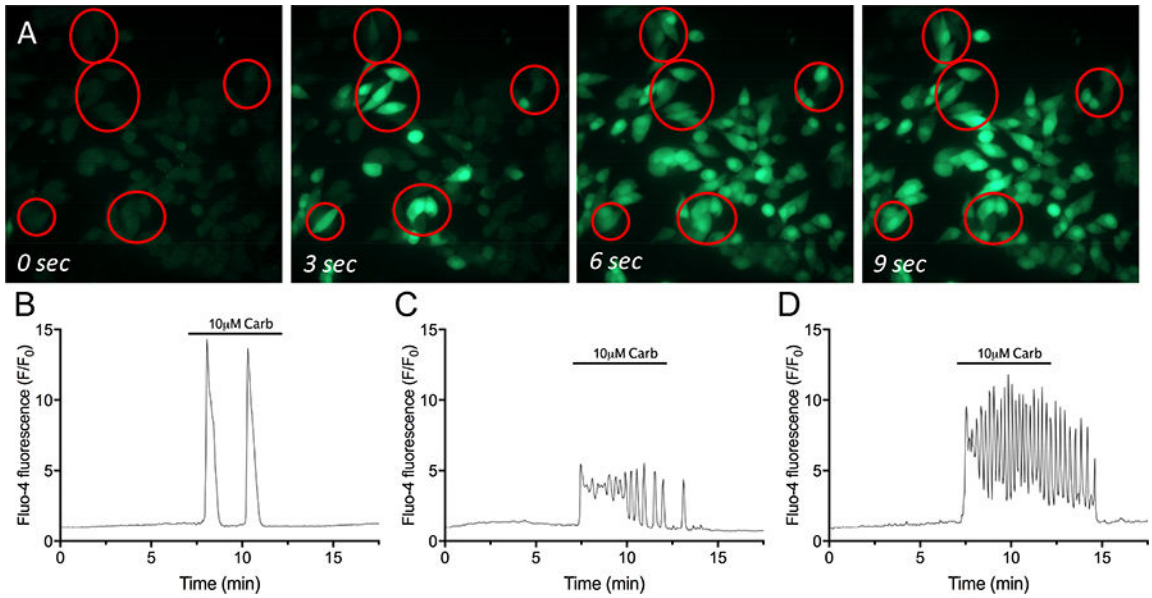

Figure 1.

(A) Representative fluorescence images taken at 3 second intervals of the same field of 10μM carbachol-treated HAC15 cells show rapid changes in Fluo-4 fluorescence. Fluorescence intensity of single, representative cells in (B), (C) and (D) during a 5-minute treatment with 10μM carbachol.

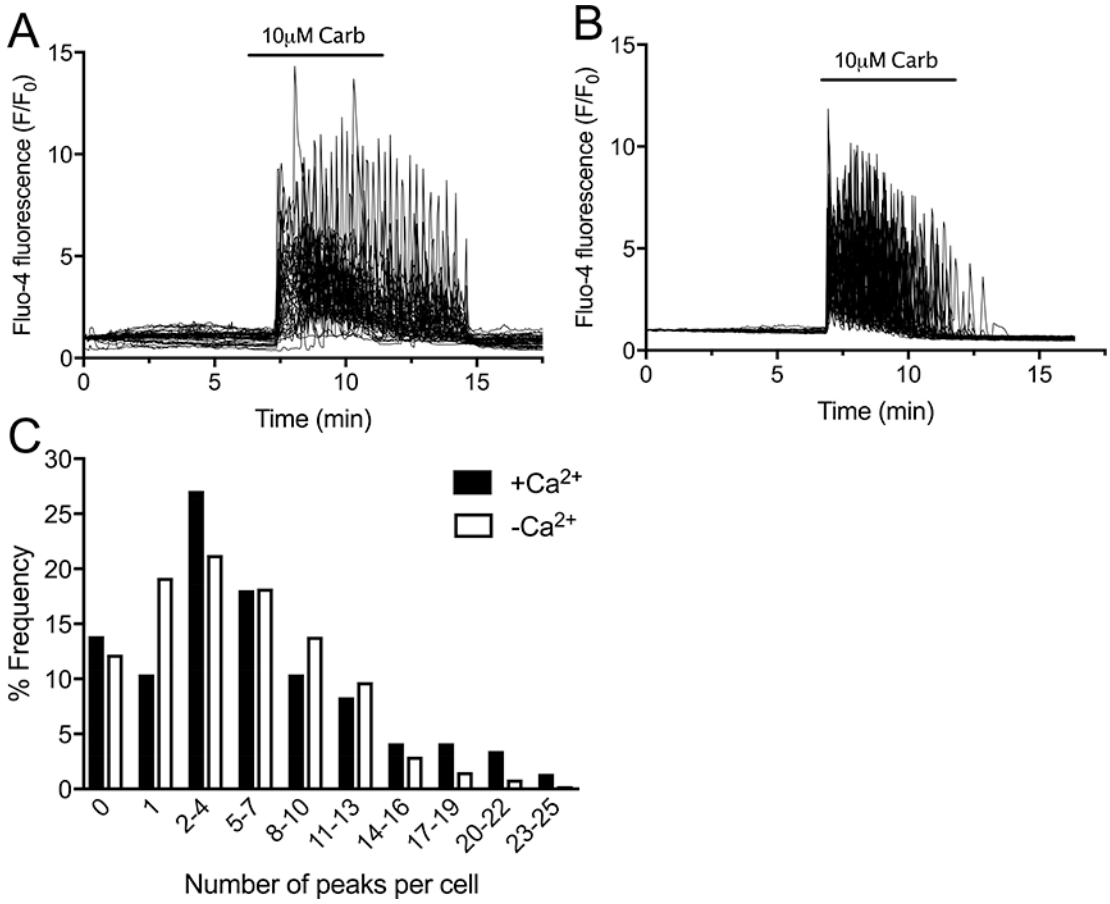

Figure 2.

Representative traces of Fluo-4 over time in HAC15 cells treated with 10μM carbachol for 5 minutes, in the presence (A) and absence (B) of extracellular Ca^{2+}. (C) Percent frequency histogram of number of peaks observed in cells from all coverslips treated with 10μM carbachol for 5 min, in the presence or absence of extracellular Ca^{2+}. N = 454 cells for $+Ca^{2+}$; 917 for - Ca^{2+}.

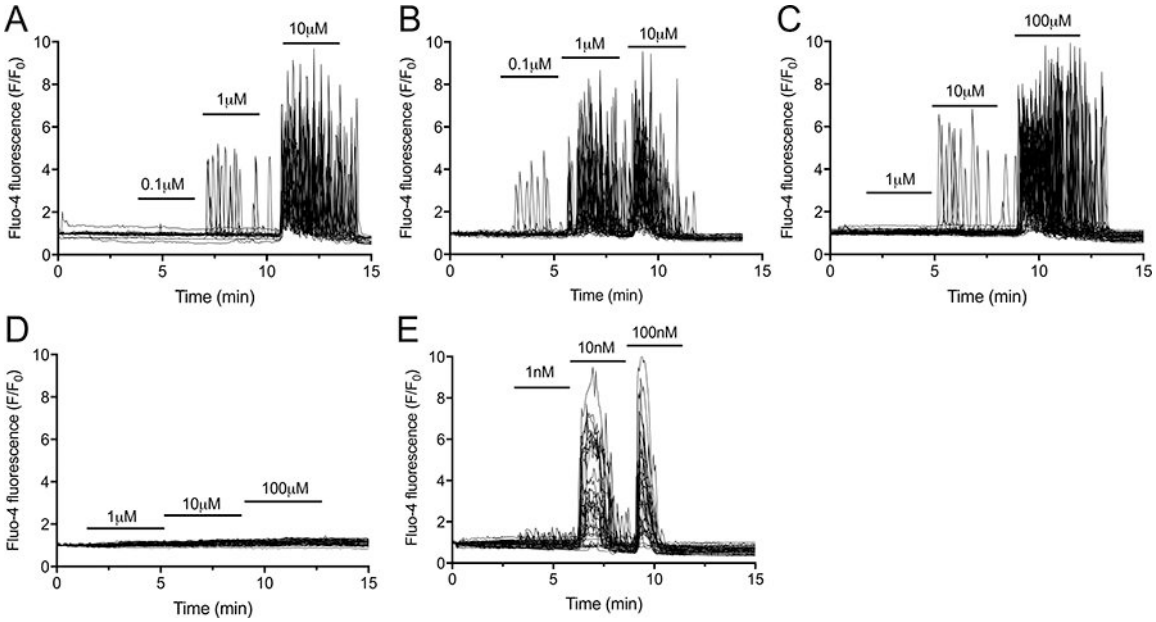

Figure 3.

Representative traces of Fluo-4 response to sequential, 3-minute additions of (A) 0.1– 10μM carbachol, (B) 0.1–10μM acetylcholine, (C) 1–100μM bethanechol, (D) 1–100μM nicotine, and (E) 1–100nM angiotensin II. Each panel shows traces from 50–100 cells from a single coverslip.

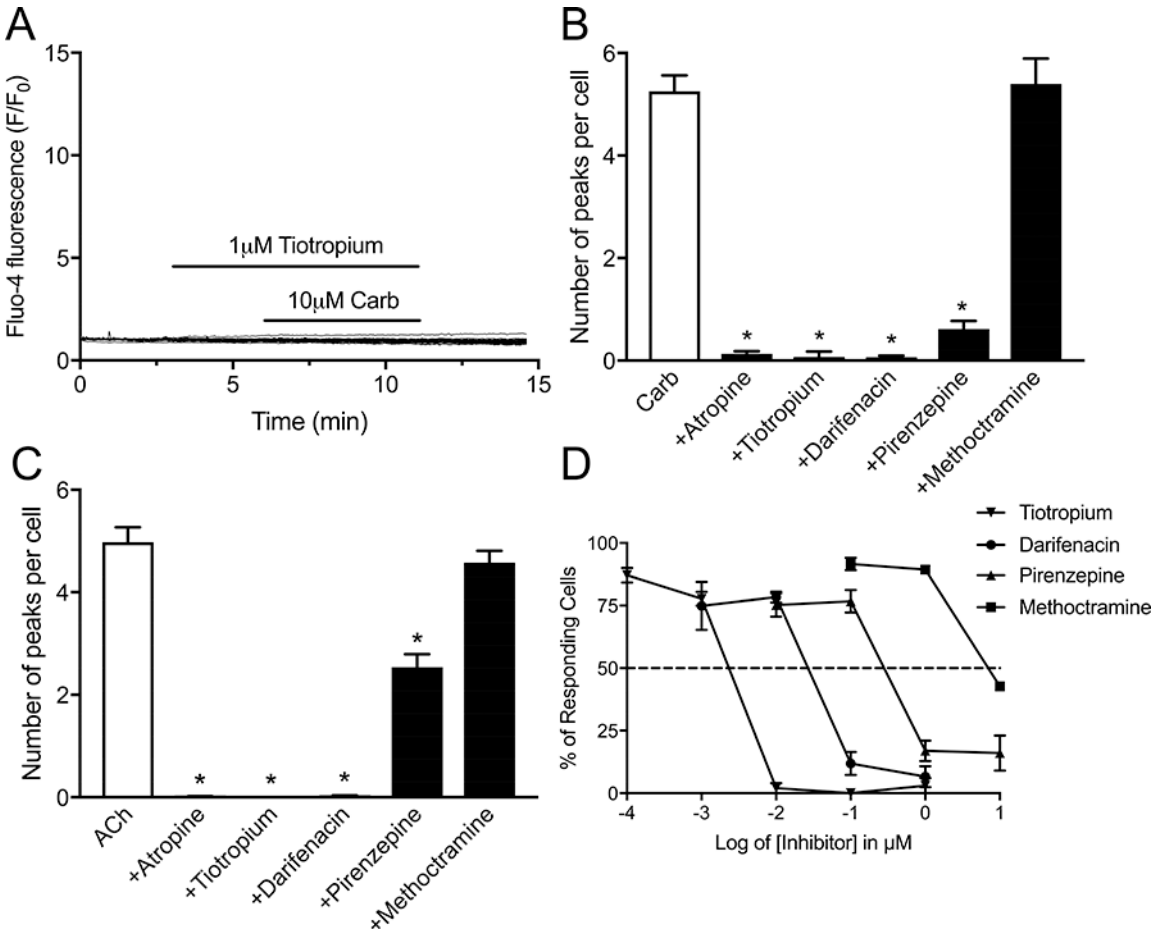

Figure 4.

(A) Representative traces of Ca^{2+} oscillations upon 5-minute exposure to 10μM carbachol in the presence of 1 μM tiotropium. Summary graphs of (B) carbachol-induced and (C) acetylcholine-induced number of peaks in cells pretreated with 1μM atropine, tiotropium, darifenacin, pirenzepine, or methoctramine. Bars represent mean number of peaks with 95% CI, for 216–917 individual cells; * $p < 0.05$. (D) Concentration-response curves show percentage of cells that responded with at least one peak (i.e. % of responding cells) in response to 10μM carbachol in the presence of muscarinic inhibitors (0.0001–10μM). Error bars represent ± SEM.

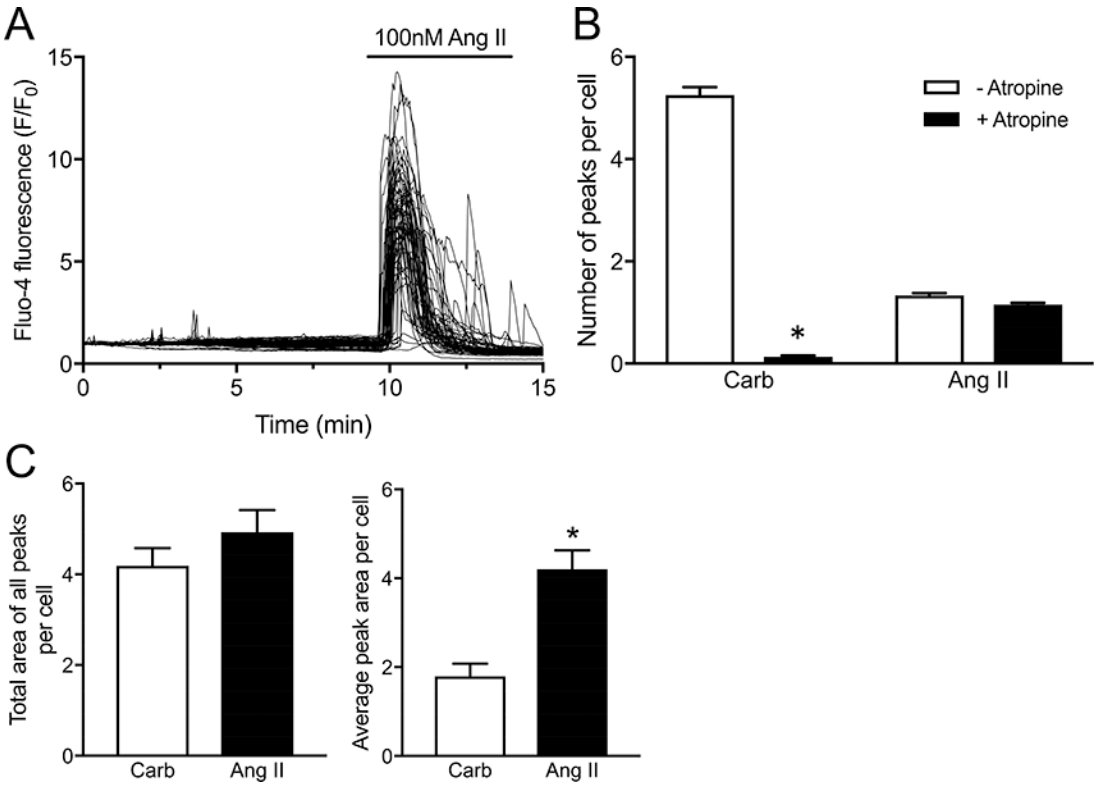

Figure 5.

(A) Representative traces of Fluo-4 changes in response to 5-minute treatment with 100nM Ang II. (B) Summary graph depicting number of peaks per cell with 10μM carbachol or 100nM Ang II with and without 1 μM atropine. (C) Comparison of carbachol vs. Ang II-treated oscillatory activity expressed as total area of all peaks for each cell, and average area for the individual peaks for each cell. Bars represent mean with 95% CI, for 170–916 individual cells. * $p < 0.05$.

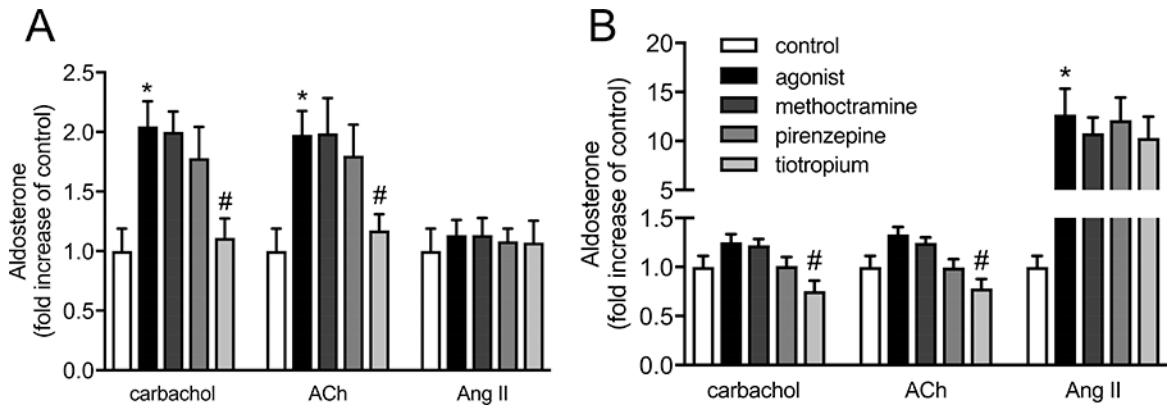

Figure 6.

Aldosterone production by HAC15 cells following 60-minute (A) or 24-hour (B) treatment with carbachol or acetylcholine (100μM), and Ang II (100nM) alone or in the presence of methoctramine, pirenzepine or tiotropium (1μM). Cells were pretreated with inhibitor for 10 minutes prior to addition of agonists. Bars represent mean aldosterone produced as a fold increase of control (unstimulated) cells ± SEM. * $p < 0.05$ in comparison to control cells; # $p < 0.05$ in comparison to cells treated with agonist alone. For each condition N=9 culture wells plated with 10^6 cells/well.

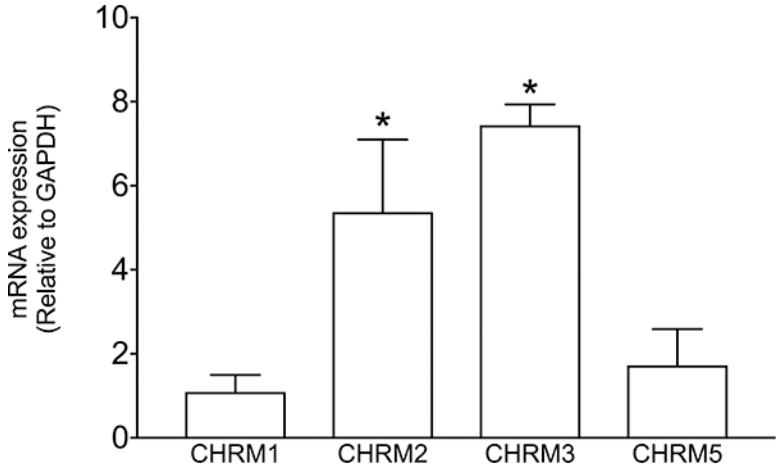

Figure 7.

Relative quantification of mRNA of muscarinic cholinergic receptor subtypes (CHRM 1, 2, 3 and 5) in HAC15 cells grown for 2 weeks in culture. Bars represent mean fold change from CHRM1 ± SEM. * $p < 0.05$. For each condition N=3 culture flasks plated with 5×10^6 cells/flask.

Table 1.

Primers used in real-time PCR reactions to detect mRNA of CHRM1–5, CYP11B1, CYP11B2, and StAR. F = forward; R = reverse.

Primer	Primer Sequence 5'–3'
$FCHRM_1$	GCTCCCCAAATACAGTCAAGAG
$RCHRM_1$	CAGCAGCAGGCGAAAGGTGT
$fchrm_2$	GATGGCCTGGAGCACAACA
$rchrm_2$	GCTGCTTAGTCATCTTCACAATC
$fchrm_3$	CGAGCAGATGGACCAAGAC
$rchrm_3$	AGGTAGAGTGGCCGTGCTC
$fchrm_4$	TCCAATGAGTCCAGCTCAGG
$rchrm_4$	AGAGCATAGCAGGCAGGGTTG
$fchrm_5$	GGACTATAAGTTCCGATTGGTG
$rchrm_5$	GGTGACTGGGACACACTTG
FCYP11B1	AGCAAGAACACGCCACAT
RCYP11B1	TTGGGAGGAGCAGGCAT
FCYP11B2	TCAAAGAGCGTCATCAGCAA
RCYP11B2	GAACTGTCACTAGAAGCCATCA
FStAR	GACCACTTTACTCATCACTTTGTC
RStAR	ACTCTCTACAGTGACCAGGAG
FGAPDH	TGTAGTTGAGGTCAATGAAGGG
RGAPDH	ACATCGCTCAGACACCATG

Table 2.

Published pK_i data for muscarinic inhibitors at M_3 and M_2 receptors; approximate selectivity, using ratio of K_is; and IC_{50} for concentration of antagonist necessary to silence oscillations in HAC15 cells treated with carbachol (10μM, 5 min). Muscarinic antagonists are ranked according to lowest to highest binding affinity to the M_3 receptor. Hegde et al., 1997; Casarosa et al., 2009.

Muscarinic Antagonists	**pK_i (M_3)**	**pK_i (M_2)**	**Fold Selectivity M_3:M_2**	**IC_{50}, in μM (in Ca^{2+}-free)**
Methoctramine	6.11	7.56	1:28	4.27
Pirenzepine	6.8	6.28	3:1	0.69
Darifenacin	8.86	7.0	73:1	0.065
Tiotropium	11.02	10.69	3:1	0.002

Table 3.

Quantitative RT-PCR of steroidogenic enzymes (CYP11B1 and CYP11B2) and transport protein (StAR) in response to 24-hour treatment with 100μM carbachol, 100μM ACh or 10^{-7}M Ang II. mRNA expression is represented as a fold increase over untreated cells ± SEM. $p < 0.05$ considered significant. For each condition N=3 culture wells plated with 10^6 cells/well.

	Carbachol		Acetylcholine		Angiotensin II	
Gene	**Fold induction**	**p value**	**Fold induction**	**p value**	**Fold induction**	**p value**
CYP11B1	1.13±0.01	0.0105	1.49±0.05	0.0065	4.31±0.08	0.0003
CYP11B2	1.26±0.01	0.0005	2.16±0.24	0.0412	15.36±0.39	0.0007
StAR	1.01±0.03	0.7487	0.98±0.03	0.6069	0.94±0.03	0.1785